Technical University of Denmark

DTU

Exergoeconomic optimization of an ammonia-water hybrid heat pump for heat supply in a spray drying facility

Jensen, Jonas Kjær; Markussen, Wiebke Brix; Reinholdt, Lars; Elmegaard, Brian

Link back to DTU Orbit

DTU Library
Technical Information Center of Denmark

Exergoeconomic optimization of an ammonia-water hybrid heat pump for heat supply in a spray drying facility

Jonas K. Jensen[a], Wiebke B. Markussen[b], Lars Reinholdt[c] and Brian Elmegaard[d]

[a] *Technical University of Denmark, Kgs. Lyngby, Denmark, jkjje@mek.dtu.dk, CA*
[b] *Technical University of Denmark, Kgs. Lyngby, Denmark, wb@mek.dtu.dk*
[c] *Danish Technological Institute, Aarhus, Denmark, lre@teknologisk.dk*
[d] *Technical University of Denmark, Kgs. Lyngby, Denmark, be@mek.dtu.dk*

Abstract:

Spray drying facilities are among the most energy intensive industrial processes. Using a heat pump to recover waste heat and replace gas combustion has the potential to attain both economic and emissions savings. In the case examined a drying gas of ambient air is heated to 200 °C. The inlet flow rate is 100,000 m^3/h which yields a heat load of 6.1 MW. The exhaust air from the drying process is 80 °C. The implementation of an ammonia-water hybrid absorption-compression heat pump to partly cover the heat load is investigated. A thermodynamic analysis is applied to determine optimal circulation ratios for a number of ammonia mass fractions and heat pump loads. An exergoeconomic optimization is applied to minimize the lifetime cost of the system. Technological limitations are applied to constrain the solution to commercial components. The best possible implementation is identified in terms of heat load, ammonia mass fraction and circulation ratio. The best possible implementation is a 865 kW heat pump with an ammonia mass fraction of 0.81 and a circulation ratio of 0.45. This results in economic savings with a present value of 177.000 € and a yearly CO_2 emissions reduction of 210 ton.

Key Words:

Spray drying, Hybrid heat pump, Exergoeconomics, High temperature heat pump, ammonia-water, Absorption

1 Introduction

Industrial spray drying facilities are among the most energy intensive industrial processes. They are applied in the production of dry solids from a liquid feedstock. This is typically needed in the chemical, pharmaceutical and food industry. Typical products of spray drying processes are powdered milk, detergents and dyes. A survey from 2005 [1] showed that the yearly energy consumption for drying operation in the United Kingdom was 348.6 PJ corresponding to 17.7 % of industrial energy consumption. Spray drying processes are typically fuelled by fossil fuel combustion, most commonly gas [1]. Therefore spray drying facilities are not only accountable for a large energy consumption but also for a large quantity of green house gas emissions. Improving the energy efficiency of spray drying facilities is thus important to reach the goals for a sustainable development of the industrial sector.

Given the recent and projected increase in renewable electricity generation from sources such as wind and solar [2], moving energy consumption from gas combustion to an electrically driven heat pump could be an environmental benefit. The implementation of heat pumps in spray drying facilities is typically restricted by the high temperature of the exhaust air (80-100 °C) which is out of the working domain for most industrial heat pumps [3]. The ammonia-water hybrid absorption-compression heat pump (HACHP) has several attributes making it applicable for high temperature operation [3, 4].

The HACHP is based on the Osenbrück cycle [5]. The first theoretical study of the HACHP was

performed by Altenkirch [6] and described the advantage of the HACHP heat pump with the non-isothermal process of absorption-desorption compared to the isothermal process of condensation-evaporation. Thereby the cycle approaches the Lorenz cycle [7] which can increase the COP by reducing the entropy generation driven by heat transfer over a finite temperature difference.

Heat pump driven drying processes has been studied by Prasertsan et al. [8], Gungor et al. [9] and Chua et al. [10]. These investigations have been limited to low temperature drying processes due the constrained heat supply temperature of conventional vapour compression heat pumps. Using a zeotropic mixture as working fluid reduces vapour pressure compared to the vapour pressure of the pure volatile component. Using the newly developed high pressure ammonia components (52 bar max. pressure) heat supply temperatures up to 150 °C can be achieved [4]. The limit for a pure ammonia system with these components is 90 °C. The development of these high pressure components and their combination with the HACHP technology has thereby shifted the working domain of industrial heat pumps making it applicable for processes like spray drying. However whether this shift allows economic and environmental savings in industry is still unanswered and should be estimated to evaluate whether heat pump development should be moved in this direction.

Ommen et al. [11] presented exergoeconomic optimization of the HACHP. This showed that the HACHP can be competitive with gas combustion and that the HACHP is the only applicable heat pump technology in the temperature range of the present study. Ommen et al. [11] tested ammonia mass fractions of 0.7 and 0.9 and found the total cost to increase with the reduction of ammonia mass fraction. This assumes constant heat transfer coefficients for the absorption and desorption. It is though well known that the heat transfer coefficient of a refrigerant mixtures is reduced due to mass diffusion resistance of the volatile component [12, 13]. This resistance is increased when the mixture composition is moved away from the pure components. This effect is thereby not accounted for in [11]. Satapathy [14] and Hultén and Berntsson [15, 16] also conclude that the ammonia mass fraction should be as high as possible, [14] concludes this based solely on exergy analysis while [15, 16] conclude this based on an evaluation of both COP and investment.

This paper will investigate the economic and environmental implication of implementing a HACHP in a spray drying facility. Using detailed heat transfer correlations the effect of changing ammonia mass fraction will be accounted for. The heat pump load, ammonia mass fraction and the circulation ratio in the HACHP will all be analysed and optimized within commercial component constraints. Combination of four ammonia concentrations and four heat pump loads will be investigated. This yields a total of 16 design conditions at which the HACHP design will be optimized. To optimize the design an exergoeconomic optimization [17, 18] is applied in each of the 16 conditions. By optimizing the design of each of the these 16 conditions the best possible design can be found and the effect of changing heat pump load and ammonia mass fraction can be evaluated without bias.

2 Method
2.1 Spray drying facility and heat pump implementation

A generic spray drying facility, as seen in Figure 1, is studied. Here ambient air is sucked into the system by an air blower at a rate of 100,000 m³/h. The air stream is first heated by a fraction of the exhaust air. Hereafter it is heated by a flue gas condenser. The ambient air has a temperature of 20 °C and a humidity ratio of 0.006 kg/kg. At the outlet of the flue gas condenser the air is 80 °C. From here the air is heated by the HACHP, utilizing exhaust air as the heat source. The air is then heated to 200 °C by a gas burner.

Heating the air from 20-200 °C results in a total heat load of 6.1 MW. The larger the HACHP load the more of the total heat load will be moved from the gas burner to the HACHP. As the exhaust temperature is uninfluenced by this: the temperature lift supplied by the HACHP increases with increasing load thus decreasing COP. It is therefore necessary to find a suitable HACHP load to ensure the viability of the investment.
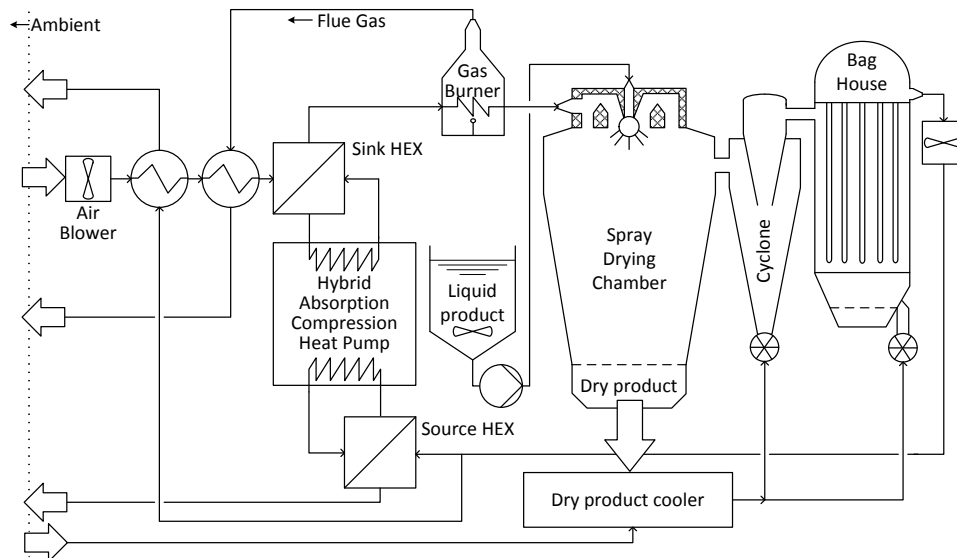
Fig. 1. Principle sketch of a generic spray drying facility

When the air has reached the target temperature of 200 °C it enters the spray drying chamber and is mixed with the atomized stream of the liquid product. This causes the liquid in the product to evaporate. The dry product can then be extracted from the bottom of the chamber. The now more humid air is passed first through a cyclone and then a bag house filter to remove left over product. Here air heated by the dry product is introduced. The exhaust air exiting the bag house has a temperature of 80 °C, humidity ratio of 0.045 kg/kg and approximately twice the mass flow rate of the drying air. This means that the capacity rate of the exhaust is higher than that of the air being heated. Therefore the exhaust stream can be split such that half can be used to heat the air directly and the rest can be used as heat source in HACHP. This in combination with the use of a flue gas condenser ensures that there is an actual heat surplus at the exhaust air temperature. Consequently the HACHP as implemented here will transfer heat across the pinch temperature [17]. The analysis and results presented in this paper is only valid for such systems. This is not always the case [19] and as a consequence of pinch analysis [17], the exhaust air is best utilized by heating the incoming air directly.

To reduce the risk of contamination two secondary circuits are used to transfer the heat between drying/exhaust air and the HACHP. The heat transfer fluid is water. On the sink side this is pressurized to prevent evaporation. The secondary circuit will increase the HACHP temperature lift, thus reducing the Coefficient of Performance (COP) but is assumed to be a necessary safety measure.

2.2 Modelling and analysis of the HACHP

The process diagram of the evaluated HACHP may be seen in Figure 2a. The process is sketched in the temperature – heat load diagram shown in Figure 2b. Here it may be seen that the profiles of the absorption and desorption processes are non-linear. This has been described in detail by Itard and Machielsen [20]. In Figure 2b these are depicted as convex curves. Dependent on the ammonia mass fraction and circulation ratio these profiles could also exhibit a concave curve or have a convex and a concave part. This is well described in Zheng et al. [21]. This means that when modelling the HACHP it is not sufficient to ensure positive temperature difference at the inlet and outlet of the absorber and desorber. To ensure a feasible profile it is necessary to verify that there is a positive temperature difference over the entire heat transfer process.

A numerical model of a HACHP has been developed in Engineering Equation Solver (EES) [22]. The thermodynamic properties of the ammonia-water mixture is calculated using equations of state developed by Ibrahim and Klein [23]. Transport properties such as viscosity and conductivity are calculated using the correlation developed by El-Sayed [24], as suggested by Thorin [25]. Each component is modelled based on a steady state mass and energy balance. Further the model ensures
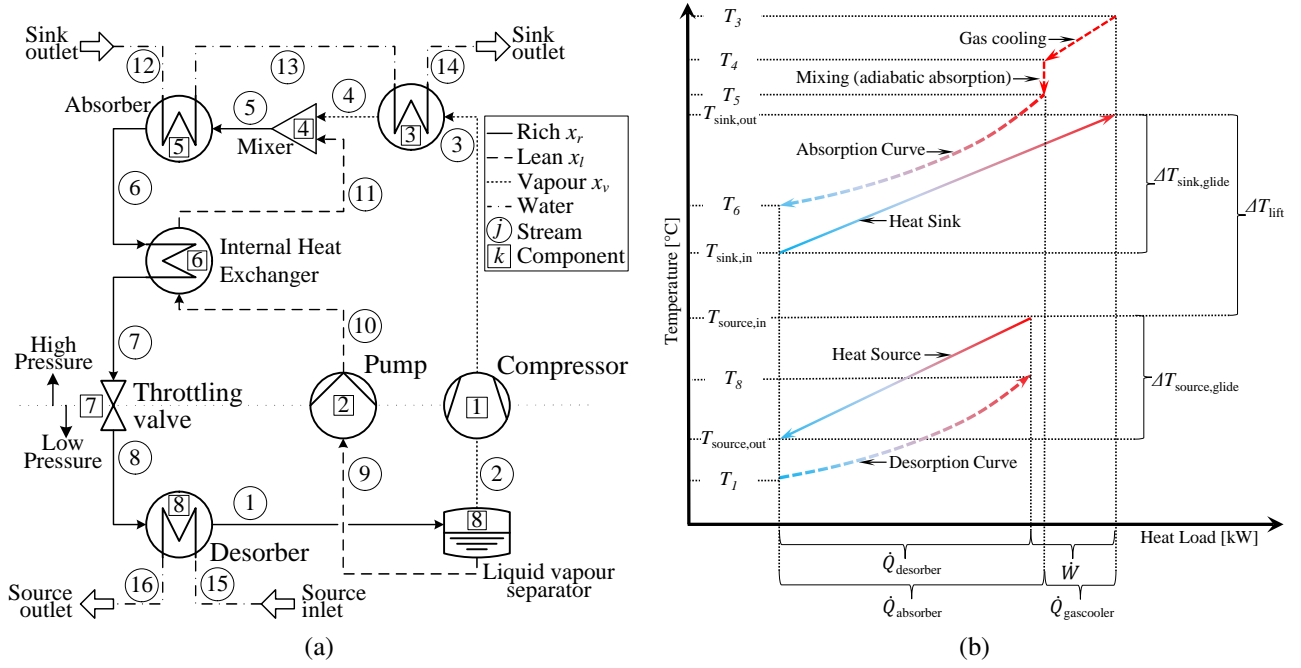
Fig. 2. (a) Principle sketch of the HACHP, (b) HACHP heat process sketched in a temperature heat load diagram

that the second law is fulfilled in all components.

The rich ammonia mass fraction x_r and circulation ratio f are inputs to the model. The rich ammonia mass fraction is present in state 5-8 and 1. The circulation ratio is defined as the ratio between the mass flow rate of the rich solution $\dot{m}_r$ and the lean solution $\dot{m}_l$: $f = \dot{m}_l/\dot{m}_r$. Hence the circulation ratio is directly linked to the vapour quality in state 1 exiting the desorber, such that: $q_1 = 1 - f$. From this is can be concluded that if the circulation ratio is 0 then the HACHP is essentially a vapour compression heat pump with a zeotropic working fluid.

Pressure and heat losses in the liquid/vapour separator are neglected, hence the temperature and pressure of stream 2 and 9 are the same as stream 1. It is assumed that the vapour and liquid exiting the separator are saturated, $q_2 = 1$ and $q_9 = 0$. The vapour and lean ammonia mass fraction, x_v and x_l, is then determined by equilibrium. The processes in the compressor and pump are modelled as adiabatic with given isentropic efficiencies, η_{is}. The transferred heat in the internal heat exchanger (IHEX) and gas cooler is calculated based on given values of effectiveness, ϵ. The mixing or adiabatic absorption process found prior to the absorber is modelled only by a mass and energy balance. Thus state 5 is the equilibrium state attained when mixing stream 4 and 11. The state exiting the absorber is assumed to be saturated, $q_6 = 0$. The forced adiabatic expansion in the throttling valve is assumed to be isenthalpic, $h_7 = h_8$.

The high and low pressures, p_H and p_L, are determined to satisfy given values of pinch point temperature difference, ΔT_{pp}, in the absorber and desorber. To account for the non-linearity of the absorption and desorption curve these processes are discretised in heat load, giving the specific enthalpy of both the sink/source and ammonia-water mixture at each step. Assuming constant pressure and constant bulk ammonia mass fraction the equilibrium temperatures and temperature differences are attained at each step. The pinch point temperature difference is defined as the minimum of these. 30 steps are used for both the absorber and desorber. The COP of the HACHP is defined as given in (1). Here $\dot{W}_1$ and $\dot{W}_2$ are the power calculated based on the given isentropic efficiencies. The efficiency of the electric motors is accounted for by the electric efficiency, η_e.

$$COP = \frac{\dot{Q}_5 + \dot{Q}_3}{\dot{W}_1/\eta_e + \dot{W}_2/\eta_e} \tag{1}$$

The displacement volume of the compressor, is found by: $\dot{V}_{\mathrm{displacement}} = \dot{V}_2/\eta_{\mathrm{vol},1}$. Here $\dot{V}_2$ is the suc-
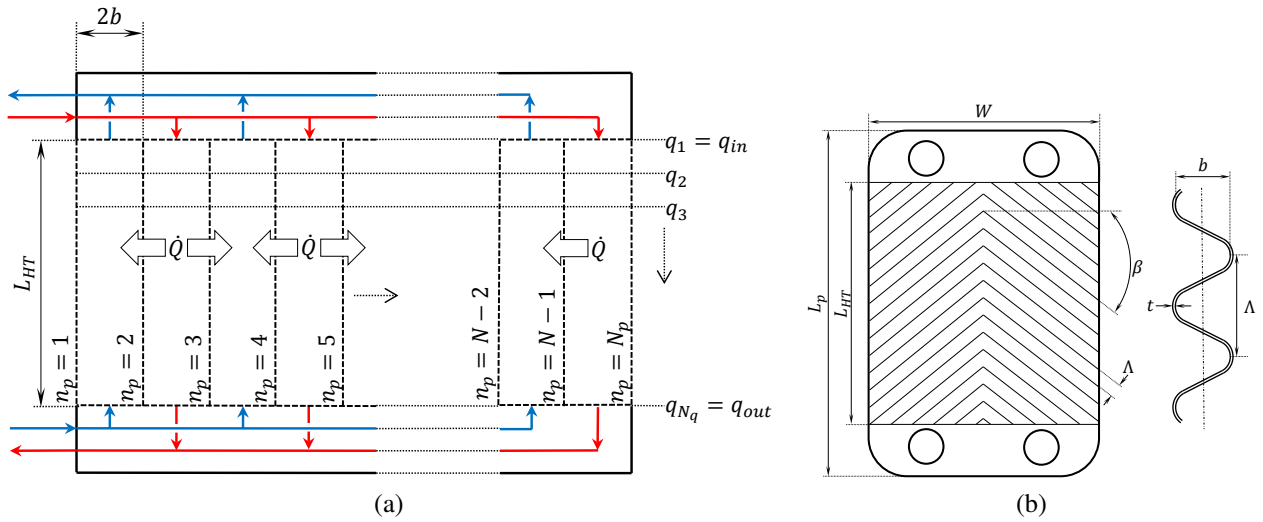
Fig. 3. (a) Principle sketch of the plate heat exchanger. (b) Plate dimension for chevron corrugation

tion line volume flow rate (calculated by the mass flow rate and specific volume of stream 2) and $\eta_{\mathrm{vol},1}$ is the volumetric efficiency of the compressor. A constant compressor and pump isentropic efficiency of 0.8 is used. The electrical efficiency of the electric motors driving the pump and compressor is 0.9. The compressor volumetric efficiency is 0.9.

It must be ensured that the system components are with in the technological limitation of commercial components. High pressure ammonia components are available up to a working pressure of 52 bar [11]. Further the compressor discharge temperature should be limited to ensure the thermal stability of the lubricant. Nekså et al. [26] state that using synthetic oil should allow discharge temperatures up to 180 °C. It is an assumption in the present study that temperatures up to 200 °C can be attained.

2.3 Heat transfer and pressure drop modelling

All heat exchangers are assumed to be of a plate type with a chevron corrugation. The use of plate heat exchangers for industrial processes have increased significantly over the last decades [27, 28] and is therefore assumed to be the preferred option for this system. The relationship between the heat load $\dot{Q}$, over all heat transfer coefficient U, temperature difference ΔT_{LMTD} and the needed heat transfer area A is given by (2). The heat loads and temperature differences are given by the HACHP cycle calculation. ΔT_{LMTD} is the logarithmic mean temperature difference and is averaged over the 30 steps of the absorber and desorber calculation. This is done to account for the non-linearity of the absorption and desorption curves. The U-value can be found as the inverse of the sum of the convective resistance of the hot and cold side and the conductive resistance in the material separating the two streams, see (2). Here α_h and α_h is the convective heat transfer coefficient of the hot and cold stream respectively, λ is the thermal conductivity of the wall material and t is the wall thickness.

$$\dot{Q} = UA\Delta T_{\mathrm{LMTD}}, \quad U = \left(\frac{1}{\alpha_h} + \frac{t}{\lambda} + \frac{1}{\alpha_c} \right)^{-1} \tag{2}$$

The working principle of a plate heat exchanger is depicted in Figure 3a. The channels in which the hot and cold fluid flows is created by the void that arises when pressing to corrugated plates against each other. The corrugation pattern may be seen in Figure 3b. Every second plate is rotated 180°, thus creating a chequered pattern of channels. By alternating the gasket placement the flow of hot and cold fluid can restricted to every second channel in a counter current arrangement. The number of channels for the hot and cold fluid is thereby related to the number of plates.

Palm et al. [29] reviewed several single and two-phase heat transfer correlations for plate exchangers and suggested that Martin's [30] is to be used. This is a semi-empirical correlation based on a heat transfer to friction analogy. Taboas et al. [31, 32, 33] have investigated the two-phase flow of ammonia-water mixtures in plate heat exchanger during desorption. This work resulted in a correla-

Table 1. Plate dimension for absorber, desorber, gas cooler and IHEX

	L_p [mm]	L_{HT} [mm]	W [mm]	β [°]	Λ [mm]	b [mm]	t [mm]	λ_p [W/mK]
Absorber & Desorber	525	456	243	60	9.6	2.5	0.4	14.06
IHEX & Gas cooler	263	228	122	60	9.6	2.5	0.4	14.06

Table 2. Applied heat transfer and pressure drop correlations for the absorber, desorber, gas cooler and IHEX

k-component	j-stream	Media		Heat transfer	Pressure drop
3 Gas cooler	13	H_2O		Martin [30]	Martin [30]
3 Gas cooler	3	NH_3/H_2O		Martin [30]	Martin [30]
5 Absorber	12	H_2O		Martin [30]	Martin [30]
5 Absorber	5	NH_3/H_2O	vapour only:	Martin [30]	
			liquid film:	Yan & Lin [37]	
			two-phase:	Silver/Bell-Ghaly [35, 36]	Yan & Lin [37]
6 IHEX	6 & 11	NH_3/H_2O		Martin [30]	Martin [30]
8 Desorber	15	H_2O		Martin [30]	Martin [30]
8 Desorber	8	NH_3/H_2O	liquid only:	Martin [30]	
			two-phase:	Taboas [31]	Taboas [31]

tion, which is applied in this study. No correlation directly addresses the two-phase flow of ammonia-water under absorption. Nordtvedt [34] suggested the use of the Silver/Bell-Ghaly method [35, 36]. Here the two-phase heat transfer coefficient is calculated based on the heat transfer coefficient of the vapour phase alone, the heat transfer coefficient of liquid film corrected is for two-phase flow effects and the gradient of the equilibrium absorption curve.

A list of the applied heat transfer and pressure drop correlations are stated in Table 2, here it is also indicated to which streams they are applied. Both heat transfer coefficient and friction factor of the two-phase flows in the absorber and desorber depend on the vapour quality q. Therefore they are discretized in q to account for this dependence. A total of 20 steps are used, and an average of the 20 values is used to estimate the U-value and friction factor.

2.4 Exergy analysis

To derive the exergy destruction in all components the specific exergy of all streams is found. The specific exergy is the sum of two contributions: a physical part e^{PH}, associated with reaching thermal and mechanical equilibrium with the dead state, and a chemical part e^{CH}, associated with reaching chemical equilibrium with the dead state [38]. The definition of physical exergy is given by (3). Here h_0 and s_0 are the specific enthalpy and entropy evaluated at the dead state T_0, p_0. The dead state in this study is chosen at T_0=25 °C and p_0=1.013 bar. The dead state enthalpy and entropy must be evaluated at the ammonia concentration of the jth stream, hence three dead state values must be calculated one for x_r, x_l and x_v respectively.

$$e_j^{PH} = h_j - h_{j,0} - T_0 \left(s_j - s_{j,0} \right) \tag{3}$$

The specific chemical exergy of an ammonia-water mixture can be calculated using (4) [17, 39]. Here $e_{NH_3}^{CH}$ and $e_{H_2O}^{CH}$ are the standard molar chemical exergy of ammonia and water respectively. At a temperature of 25 °C and pressure of 1.013 bar these attain values of $e_{NH_3}^{CH}$ = 336684 kJ/kmol and $e_{H_2O}^{CH}$ = 45 kJ/kmol [17]. Further $w_{X_j}^{rev}$ is the reversible specific work associated with the mixing of pure ammonia and pure water [39]. Again one value of specific chemical exergy must be calculated for each of the three concentrations in the system.

$$e_j^{CH} = x_j e_{NH_3}^{CH} + (1 - x_j) e_{H_2O}^{CH} + w_{X_j}^{rev} \tag{4}$$
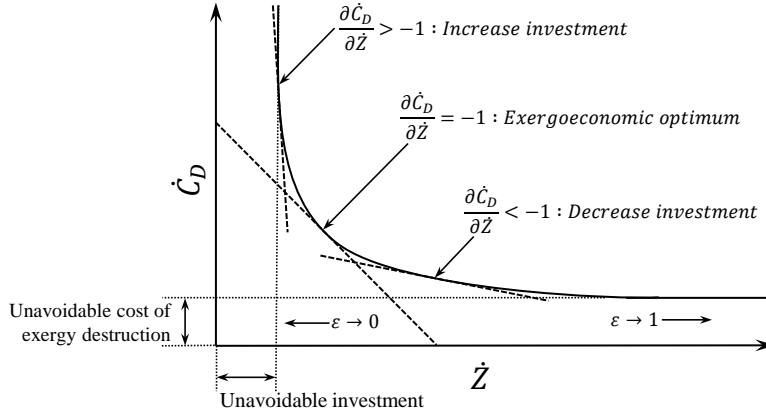
Fig. 4. Graphical representation of the exergoeconomic optimum

Table 3. Definition of exergy fuel and product and fuel and product cost

k^{th}	Component	$\dot{E}_{F,k} =$	$\dot{E}_{P,k} =$	$\dot{C}_{F,k} =$	$\dot{C}_{P,k} =$
1	Compressor	$\dot{W}_1$	$\dot{E}_3 - \dot{E}_2$	$c_w \dot{W}_1$	$\dot{C}_3 - \dot{C}_2$
2	Pump	$\dot{W}_2$	$\dot{E}_{10} - \dot{E}_9$	$c_w \dot{W}_2$	$\dot{C}_{10} - \dot{C}_9$
3	Gas cooler	$\dot{E}_3 - \dot{E}_4$	$\dot{E}_{14} - \dot{E}_{13}$	$\dot{C}_3 - \dot{C}_4$	$\dot{C}_{14} - \dot{C}_{13}$
5	Absorber	$\dot{E}_5 - \dot{E}_6$	$\dot{E}_{13} - \dot{E}_{12}$	$\dot{C}_5 - \dot{C}_6$	$\dot{C}_{13} - \dot{C}_{12}$
6	IHEX	$\dot{E}_6 - \dot{E}_7$	$\dot{E}_{11} - \dot{E}_{10}$	$\dot{C}_6 - \dot{C}_7$	$\dot{C}_{11} - \dot{C}_{10}$
8	Desorber	$\dot{E}_{15} - \dot{E}_{16}$	$\dot{E}_1 - \dot{E}_8$	$\dot{C}_{15} - \dot{C}_{16}$	$\dot{C}_1 - \dot{C}_8$
System		$\dot{E}_{F,1} + \dot{E}_{F,2} + \dot{E}_{F,8}$	$\dot{E}_{P,3} + \dot{E}_{P,5}$	$\dot{C}_{F,1} + \dot{C}_{F,2} + \dot{C}_{F,8}$	$\dot{C}_{P,3} + \dot{C}_{P,5}$

$$w_{X_j}^{\text{rev}} = \left(h_{j,0} - x_j h_{\text{NH}_3,0} - (1 - x_j) h_{\text{H}_2\text{O},0} \right) - T_0 \left(s_{j,0} - x_j s_{\text{NH}_3,0} - (1 - x_j) s_{\text{H}_2\text{O},0} \right) \tag{5}$$

When the specific exergy of all streams are calculated the total exergy flow rate associated with each stream can be calculated as the product of the specific exergy of the $j'th$-stream an it's corresponding mass flow rate: $\dot{E}_j = \dot{m}_j \left(e_j^{\text{PH}} + e_j^{\text{CH}} \right)$.

The control volumes surrounding the compressor and pump are assumed to be adiabatic and therefore exchange only mass and work. The remaining components are assumed to be surrounded by an adiabatic and zero-work boundary and thus all transferred exergy is related to the transfer of material streams. For components in which an exergetic fuel and product can be defined the exergy destruction can be found as the difference between these two: $\dot{E}_{D,k} = \dot{E}_{F,k} - \dot{E}_{P,k}$. For these components the product and fuel definitions may be seen in Table 3. Components such as the mixer and the throttling valve are dissipative components. Therefore a meaningful exergetic fuel and product cannot be defined. For these two components the exergy destruction can be found by applying an exergy balance to the component control volume: $\dot{E}_{D,4} = \dot{E}_5 - (\dot{E}_4 + \dot{E}_{11})$ and $\dot{E}_{D,7} = (\dot{E}_7 - \dot{E}_6)$.

To evaluate the exergetic performance of the components an exergy efficiency ε is defined,(6) [17]. Further two exergy destruction ratios are defined: y_k and y_k^* (6) [17]. y_k is the exergy destruction in the kth component relative to the total exergy fuel supplied to the system. y_k^* is the exergy destruction in the kth component relative to the total exergy destruction in the system.

$$\varepsilon_k = \frac{\dot{E}_{P,k}}{\dot{E}_{F,k}}, \quad y_k = \frac{\dot{E}_{D,k}}{\dot{E}_{F,\text{tot}}}, \quad y_k^* = \frac{\dot{E}_{D,k}}{\dot{E}_{D,\text{tot}}} \tag{6}$$

2.5 Exergoeconomic analysis and optimization

The exergoeconomic analysis and optimization is a method for estimating and minimizing the total cost of an energy conversion system over the course of it's lifetime. The total cost is comprised of two contributions: the system investment cost and the cost of operating the system. The cost of

operating the system can be linked to the cost of the system's exergy destruction. Meaning that what is paid for converting the exergy fuel to the exergy product is the specific unit cost of the exergy fuel multiplied by the amount of exergy fuel that is not converted to the exergy product (exergy destruction). This means that if the exergy efficiency of the system is increased the operation cost is reduced. Increasing exergy efficiency typically requires increased investment. E.g. for a heat exchanger the exergy efficiency is increased if the temperature difference is reduced, consequently the heat transfer and subsequently the investment must increased to adapt to the reduced thermal potential. This behaviour is depicted in Figure 4. Here it may be seen that the relation of $\dot{C}_D$ to $\dot{Z}$ has a horizontal and vertical asymptote. For an infinite investment some exergy destruction will prevail, this is known as the unavoidable exergy destruction [40]. Further, no matter how much the exergy efficiency is decreased some investment will be needed, this is known as the unavoidable investment [40]. This behaviour limits the use of the conventional exergoeconomic optimization as this uses indicators based on absolute values of $\dot{C}_D$ and $\dot{Z}$ and thus does not account for the unavoidable parts.

In the present study cost functions for the component's Product Equiptment Cost (PEC) are used. Therefore the investment cost can be expressed mathematically as function of the HACHP design. This also allows the exergoeconomic optimum to be defined mathematically. As seen in Figure 4 the exergoeconomic optimum is defined where the marginal cost rate of the levelized investment cost $\dot{Z}$ is equal to the marginal cost rate of exergy destruction $\dot{C}_D$. This means that the optimum is obtained when $d\dot{C}_D/d\dot{Z} = -1$. Subsequently, if $d\dot{C}_D/d\dot{Z} > -1$ the total cost can be reduced by increasing the exergy efficiency at the expense of an increased investment. Conversely if $d\dot{C}_D/d\dot{Z} < -1$ the total cost is reduced by reducing the investment at the expense of a reduced exergy efficiency.

The design of the HACHP is governed by four decision variables. These are ΔT_{pp} for the absorber and desorber and ϵ of the IHEX and gas cooler. A change in these variables will all exhibit the behaviour represented in Figure 4. It is the objective of the exergoeconomic optimization to determine the optimum values of these four variables. This has been done by an iterative optimization procedure. Initial guess values for the four variable have been made. Using the "Uncertainty Propagation" procedure in EES [22] the partial derivatives of both the investment cost and the operation cost can be found with respect to the four decision variables individually. Based on these partial derivatives it can be decided whether to increases or decrease the values. E.g. if: $\delta\dot{C}_D^\Sigma/\delta\Delta T_{\mathrm{pp},5} > \delta\dot{Z}^\Sigma/\delta\Delta T_{\mathrm{pp},5}$ the absorber pinch point temperature difference should be reduced. The superscript Σ here indicates that it is the total system investment cost rate and the total system exergy destruction cost rate rather than the component costs rates. This ensures that the component interdependencies are accounted for. This procedure has been repeated until $d\dot{C}_D^\Sigma/d\dot{Z}^\Sigma \in \{-0.9, -1.1\}$ for all the four decision values simultaneously, at which the optimum is said to be attained.

In order to conduct this optimization the exergy cost rate, $\dot{C}_j$, of all stream must be determined. This is done by applying cost balances to all components. The general form of a component cost balance is seen in (7) [17, 18].

$$\sum_e \left(c_e \dot{E}_e\right)_k + c_{w,k}\dot{W}_k = c_{q,k}\dot{E}_{q,k} + \sum_e \left(c_i \dot{E}_i\right)_k + \dot{Z}_k \tag{7}$$

Seven auxiliary relations are needed to determine the exergy cost rates. It is a general assumption that the specific unit cost of exergy for the hot stream of a heat exchanger above dead state temperature is unchanged [17]: $c_3 = c_4$, $c_5 = c_6$, $c_6 = c_7$, and $c_{15} = c_{16}$. Further it is assumed that the specific unit cost of exergy of the vapour stream and liquid stream exiting the liquid/vapour separator are equal: $c_2 = c_9$. No cost is affiliated with the inlet condition of the sink and source: $c_{12} = c_{15} = 0$.

The definition of the fuel and product cost for the non dissipative components and for the total HACHP system are stated in Table 3. Using these definitions the component specific fuel, $c_{F,k}$ and product, $c_{P,k}$ cost can be determined, (8). Further the conventional exergoeconomic indicators are determined, see (8). These are the exergoeconomic factor f_{ex}, indicating the non-exergetic cost's impact on the the total cost and the relative cost difference r indicating the relative increase in cost between the fuel

and product of a component.

$$c_{F,k} = \frac{\dot{C}_{F,k}}{\dot{E}_{F,k}}, \quad c_{P,k} = \frac{\dot{C}_{P,k}}{\dot{E}_{P,k}}, \quad f_{ex,k} = \frac{\dot{Z}_k}{\dot{Z}_k + c_{F,k}\dot{E}_{D,k}} \quad r_k = \frac{c_{P,k} - c_{F,k}}{c_{F,k}} \tag{8}$$

PEC cost functions have been developed based on Danish intermediate trade business prices [41, 42] and individual producers [43]. The cost function are constructed as proposed by Bejan et al. [17]. A number of assumptions have been made to estimate the total investment of the HACHP system. These are as follows:

- Total capital investment of a component is 4.16 higher than the PEC of the component [17].

- PEC for a compressor is a function of the compressor displacement volume.

- PEC for an electrical motor with a fixed efficiency is dependent only on the shaft power.

- PEC for a heat exchanger is a function of the heat exchange area.

- PEC of the pump is equivalent to it's electrical motor.

- PEC of the expansion valve, mixer and the liquid vapour separator are neglected.

To determine the levelized capital component cost rates the capital recover factor [17] is used. An interest rate of 7% and inflation rate of 3% are assumed, further the technical life time is 15 years with 3000 operating hours per year. The component's maintenance cost rate is assumed to be 20% of the levelized capital cost rates. The total non-exergetic cost rate is the sum of the capital investment and maintenance cost rate. Electricity and natural gas prices correspond to an industrial process consumer in the Danish fiscal environment, prices are found in [2].

3 Results

3.1 Thermodynamic analysis

The ammonia mass fraction of the rich solution and the circulation ratio both have great influence of both the COP and the pressure levels in the system. As described by Jensen et al. [4] and Zamjlrescu [44] it is important to find the correct combination of the these two parameters. Figure 5 shows the COP of the HACHP as a function of the ammonia mass fraction x_r and circulation ratio f with $\Delta T_{\text{pp},5} = \Delta T_{\text{pp},8} = 10$ K and $\epsilon_3 = \epsilon_6 = 0.7$. Figure 5a is for a HACHP covering 10 % of the total heat load of 6.1 MW. Figure 5b is for 15%, 5c for 20 % and 5d is 25 % of the heat covered by the heat pump. The solution with $x_r < 0.55$ are discarded as these tend to result in sub-atmospheric desorber pressures and large volumetric flow rates in the compressor [4]. It is seen that for all four load shares in the range of $x_r > 0.55$ one circulation ratio optimizes the COP for each value of x_r. The optimum COP line for all four loads are shown with the dashed line. It can be seen that this line shifts downward as the HACHP load is increased. Hence the higher the load the lower the circulation ratio should be. Four points are chosen at each HACHP load, these are with an x_r of 0.6, 0.7, 0.8 and 0.9 and the corresponding optimum circulation ratio. These points are indicated with circles on Figure 5.

3.2 Exergoeconomic optimization

The exergoeconomic analysis can then be applied to determine the exergoeconomic optimum design at the 16 points derived from the thermodynamic analysis. Table 4 shows the result of the exergoeconomic analysis at an initial set of guess values and at the exergoeconomic optimum respectively. Both with a HACHP load of 15 % and a rich ammonia mass fraction x_r=0.8. The initial guess values are $\Delta T_{\text{pp},5} = \Delta T_{\text{pp},8} = 15$ K and $\epsilon_3 = \epsilon_6 = 0.9$. As may be seen in Table 4 for the initial guess values total cost rate for the gas cooler is the third highest only surpassed by the compressor and absorber. The gas cooler also has the second highest relative cost difference. Judging from the low exergoeconomic
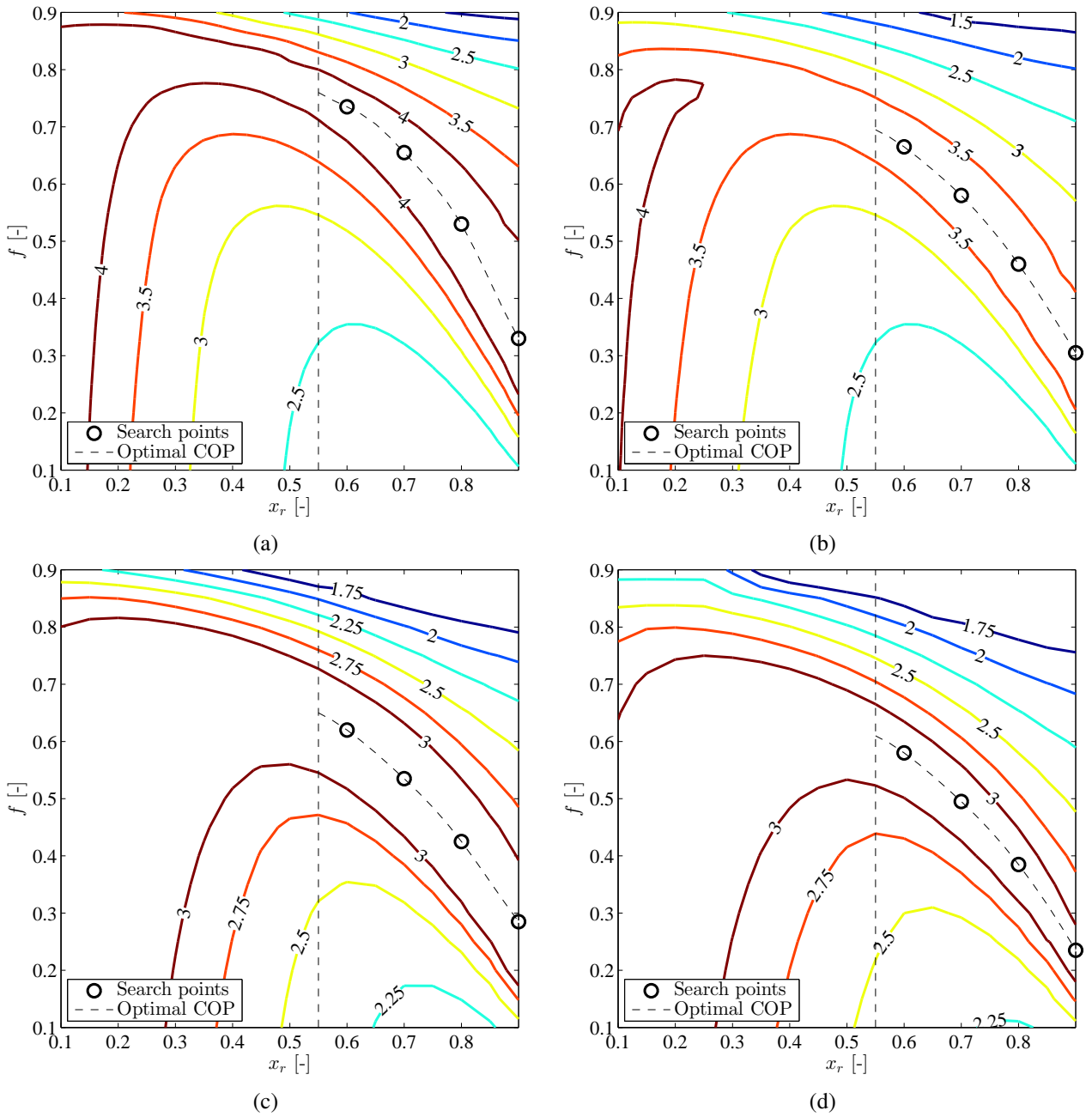
Fig. 5. COP of the HACHP as function of x_r and f for a HACHP covering (a): 10 %, (b): 15 %, (c): 20 % and (d): 25 % of the total heat load.

factor conventional exergoeconomic optimization states that the investment here should be increased but judging from the partial derivative the investment should actually be decreased to reduce the over all cost. This difference arises as the partial derivative method accounts for both the interdependencies between component exergy efficiencies and for the unavoidable part of exergy destruction and investment. In the case of the absorber and IHEX it may be seen that the conclusions of the conventional exergoeconomic optimization and the partial derivative method coincide. It should be noted that the exergoeconomic factor for the desorber is $f_{ex,8}$=1. This is because no cost is associated with the waste heat and thus $c_{F,k}$=0. Therefore the relative cost difference can not be calculated as $c_{F,k}$ is the fraction denominator. This makes it hard to judge whether or not the choice of the design parameter for the desorber is appropriate. However judging from the partial derivative it is clear that savings to the over all cost can be attained by reducing the exergy destruction in the desorber.

The conclusion from the partial derivatives of the initial guess is that: The effectiveness of the IHEX and gas cooler should be reduced to lower the investment, the IHEX effectiveness should be lowered

more than the gas cooler. Further the absorber and desorber pinch point temperature difference should both be reduced, the desorber's more than the absorber's.

Table 4 states the cost rates and exergoeconomic indicators at the optimum decision values suggested by the partial derivatives method. Here the absorber and desorber pinch point temperature differences are reduced to 12.6 K and 10.4 K, respectively. The IHEX effectiveness is reduced to 0.69 and the gas cooler effectiveness to 0.87. Hence the direction and the magnitude of the change in variables is consistent with the conclusion of the partial derivatives from the initial guess. Further it can be seen that only the exergoeconomic factor and relative cost difference of the IHEX undergo substantial change between the initial guess and the optimum. This emphasizes the difficulty of determining the exergoeconomic optimum using the conventional exergoeconomic procedure. The present value of the savings attained by the HACHP is 120,000 € with the initial guess values. This is increased by 43 % at the exergoeconomic optimum to a value of 172,000 €. The physical variables of the HACHP process for the exergoeconomic optimum from Table 4 are listed in Table 5.

This optimization procedure has been conducted for all of the 16 design configurations. Figure 6a shows the components PEC of all 16 optimal designs. While Figure 6b shows the total lifetime cost of operating (TCO) the component. This is the present value of the exergy destruction cost over the system's lifetime. The system fuel cost is used so that the cost of operating the dissipative components can be estimated. It may be seen that the total PEC increases when decreasing the ammonia mass fraction. This is caused by an increase in the compressor, IHEX and desorber PEC. The remaining components are indifferent to the change in ammonia mass fraction. The compressor PEC increases the most. This is caused by the reduced vapour pressure of the working fluid resulting in an increased displacement volume. The IHEX PEC is increased as the circulation ratio is increased for reduced ammonia mass fractions. Thereby the capacity rates of the rich and lean mixtures approach each other, consequently reducing the mean temperature difference and increasing the needed heat load. Both resulting in the need for an increased area. Figure 6a also shows that the total PEC increases when the heat pump load is increased, the marginal PEC cost is close to constant.

From Figure 6b it is seen that also the cost of operating the system increases when decreasing the ammonia mass fraction. It is seen that the cost of operating the compressor is not significantly influenced by the ammonia mass fraction. Further the gas cooler operation cost is indifferent to x_r for HACHP loads of 10% and 15%. The throttling valve on the other hand is not influenced by x_r at 20% and 25%. For the mixing, absorber and IHEX the cost of operation is increased, when decreasing the ammonia mass fraction. For the absorber this is caused by the degradation of the two-phase heat transfer coefficient. The reduced heat transfer coefficient shifts the optimal size of the absorber to a higher exergy destruction rate. For the mixing and the IHEX the increased operational cost is caused by the increased circulation ratio. For the desorber the opertional cost decreases when the ammonia mass fraction is reduced. This, in spite of the decreased heat transfer coefficient and is caused by the interdependency between the low pressure and the compressor investment. Hence a larger desorber investment can reduce the compressor investment as the low suction line pressure is increased. Further the total cost of operating the system increases as the load is increases, the marginal TCO increase with the HACHP load.

3.3   HACHP implementation, economic and environmental savings

Several issues govern the implementation of the HACHP. As shown in Fig. 6, both the choice of ammonia mass fraction and heat pump load influence the investment and the operating costs of the HACHP. To estimate yearly CO_2 emissions the fuel specific emission factors for electricity and natural gas in the Danish energy system is used [2].

Figure 7 shows the economic and CO_2 savings as well as the compressor discharge temperature and pressure. All are shown as a function of the HACHP load $\dot{Q}_{HP}$. Legends indicate the ammonia mass fraction. The values are given for the exergoeconomic optimum designs. Figure 7a shows the present

Table 4. Non exergetic and exergetic cost rates and exergoeconomic indicators for the initial guess and optimal solution for a HACHP with x_r=0.8 covering 15 % of the total heat load.

k^{th}	Component	Initial guess variables				exergoeconomic optimum			
		$\dot{Z}_k + \dot{C}_{D,k}$	$f_{ex,k}$	r_k	$\frac{\delta \dot{C}_D^\Sigma}{\delta \dot{Z}^\Sigma}$	$\dot{Z}_k + \dot{C}_{D,k}$	$f_{ex,k}$	r_k	$\frac{\delta \dot{C}_D^\Sigma}{\delta \dot{Z}^\Sigma}$
		[¢/h]	[-]	[-]		[¢/h]	[-]	[-]	
1	Compressor	673	0.64	0.40	-	651	0.65	0.41	-
2	Pump	14.7	0.59	0.53	-	14.5	0.60	0.54	-
3	Gas Cooler	339	0.086	0.62	-0.40	283	0.094	0.59	-1.02
4	Absorber	364	0.27	0.25	-1.6	362	0.38	0.25	-1.05
6	IHEX	204	0.76	0.95	-0.21	72.1	0.46	0.52	-0.96
8	Desorber	74.8	1.0	-	-2.9	163	1.0	-	-0.95

Table 5. Thermodynamic state point variables for the exergoeconomic optimum seen in Table 4, x_r=0.8 and 15 % of the total heat load covered by HACHP.

| j^{th}	$\dot{m}_j$	p_j	T_j	x_j	h_j	s_j	$v_j \cdot 10^{-3}$	e^{PH}	e^{CH}
	[kg/s]	[bar]	[°C]	[-]	[kJ/kg]	[kJ/kgK]	[m³/kg]	[kJ/kg]	[kJ/kg]
1	1.39	13.04	63.40	0.80	774.0	2.80	62.3	218.8	15875
2	0.752	13.04	63.40	0.99	1385	4.52	114	357.2	19766
3	0.752	50.21	200.2	0.99	1674	4.65	41.5	609.7	19766
4	0.752	50.21	126.4	0.99	1426	4.09	31.0	526.4	19766
5	1.39	50.21	120.4	0.80	856.0	2.75	14.8	317.2	15875
6	1.39	50.21	101.8	0.80	362.0	1.45	1.72	208.7	15875
7	1.39	50.21	91.10	0.80	304.0	1.30	1.67	197.7	15875
8	1.39	13.04	44.70	0.80	304.0	1.36	22.8	177.6	15875
9	0.641	13.04	63.40	0.57	57.00	0.775	1.40	55.73	11308
10	0.641	50.21	64.50	0.57	63.00	0.779	1.32	60.77	11308
11	0.641	50.21	90.70	0.57	187.0	1.13	1.38	79.44	11308
12	7.89	5.000	85.00	-	356.0	1.13	-	22.72	-
13	7.89	5.000	105.7	-	444.0	1.37	-	39.36	-
14	7.89	5.000	111.3	-	467.0	1.43	-	44.52	-
15	7.89	5.000	75.00	-	314.0	1.02	-	16.19	-
16	7.89	5.000	55.20	-	231.0	0.770	-	6.386	-
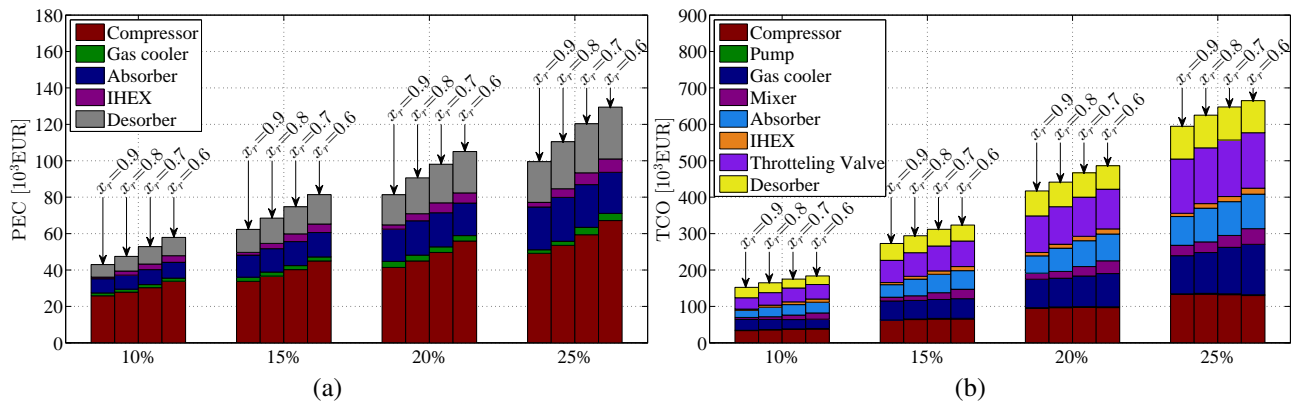
Fig. 6. (a) Product equipment cost of the $k'th$-component at HPLS of 10%, 15%, 20% and 25% and x_r of 0.6, 0.7, 0.8 and 0.9. (b) Present value of the the $k'th$-component's exergy destruction cost over the HACHP lifetime at HPLS of 10%, 15%, 20% and 25% and x_r of 0.6, 0.7, 0.8 and 0.9
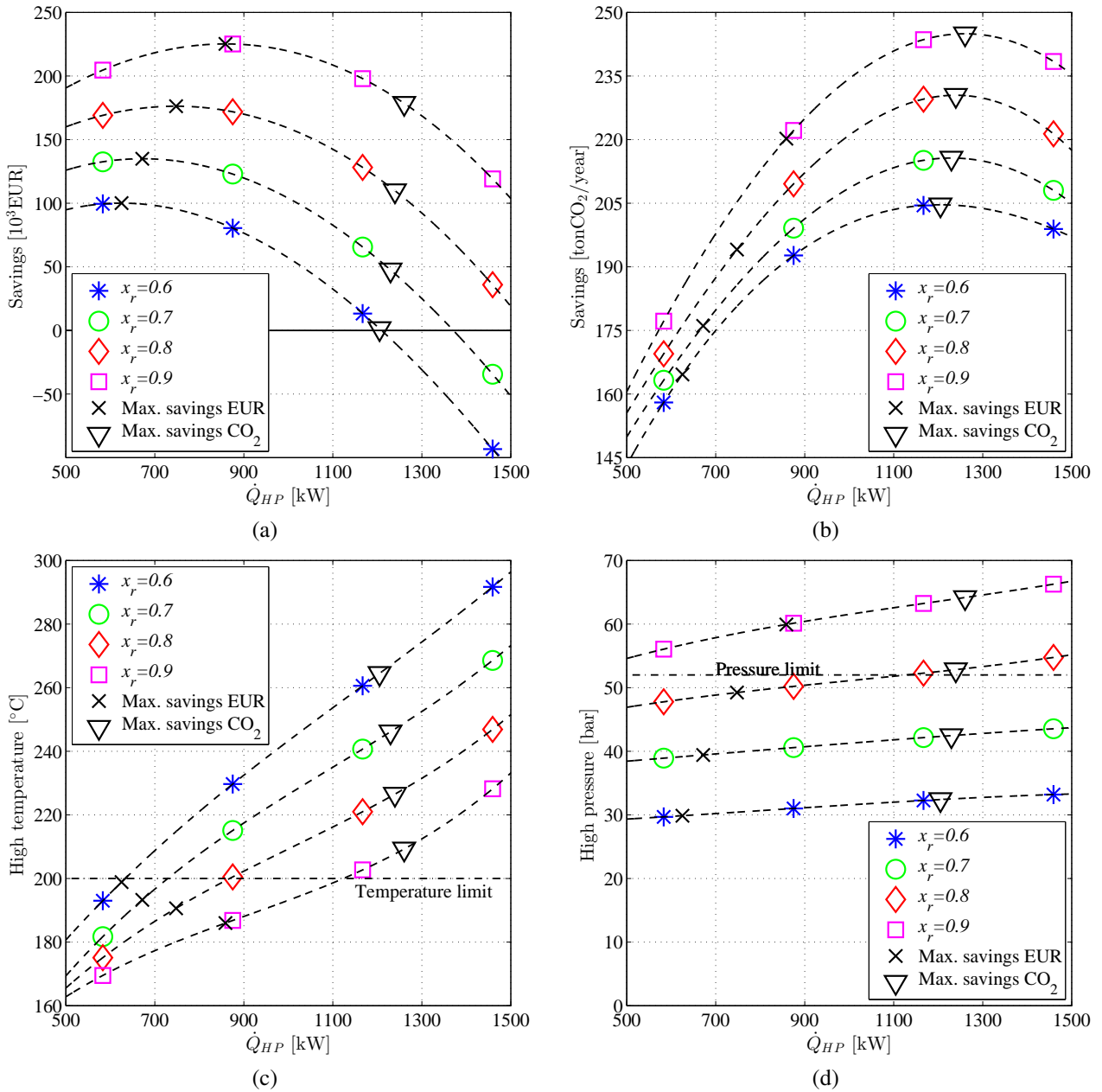
Fig. 7. (a) Present value of the economic savings. (b) Yearly CO_2 emission savings. (c) Compressor discharge temperature. (d) Compressor discharge pressure. All shown a function of the design heat pump load and ammonia mass fraction.

value of the economic savings in €. As may be seen: for each ammonia mass fraction there is one heat pump load that maximize the savings. This is the point at which the marginal total cost of the HACHP (investment plus operation) is equal to the marginal cost of gas heating. As seen the higher the ammonia mass fraction the higher the savings and the higher the optimum HACHP load. Figure 7b shows the yearly CO_2 emissions savings. It may here be seen that the maximum emissions savings occurs a higher HACHP load than the maximum economic savings. Again it is seen that the higher the ammonia mass fraction the higher the emissions savings.

Figure 7c shows the compressor discharge temperature and the temperature limit. It may be seen that none of the economic optimum loads are restricted by the temperature limit. While all of the optimum emission loads are beyond the maximum temperature. Further it can be seen that increasing the ammonia mass fraction decreases the compressor discharge temperature. Figure 7d shows the compressor discharge pressure. Here it may be seen that only the optimal savings for x_r=0.9 is restricted by the pressure limit. Further is may be seen that increasing the ammonia mass fraction
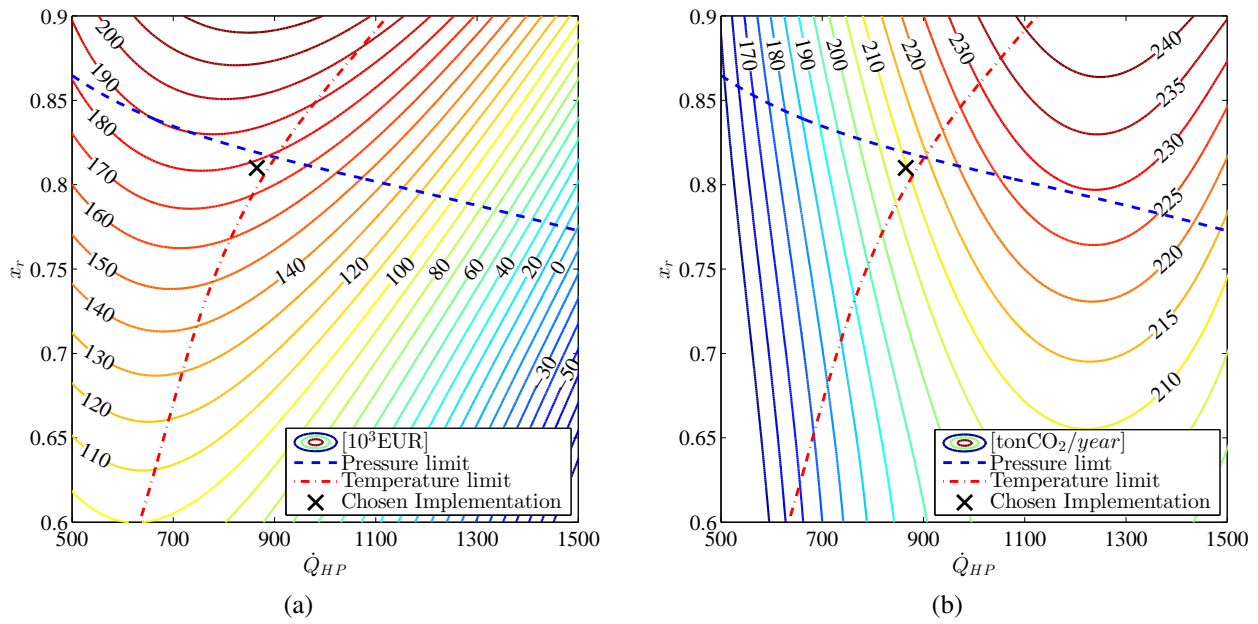
Fig. 8. (a) Interpolation of the economic savings. (b) Interpolation of the emission savings. Both as a function of the design heat load and ammonia mass fraction and with compressor discharge pressure and temperature limit imposed.

increases the discharge pressure.

As the best possible implementation of the HACHP may be one with an ammonia mass fraction between the curves shown in Figure 7: an interpolation between HACHP load and the ammonia mass fraction for the 16 exegoeconomic optimum points has been made. Figure 8a shows the interpolation of economic savings with the pressure and temperature limits imposed. The area below the blue dashed line satisfies the pressure constraint, while the area to the left of the red dash-dot line satisfies the temperature constraint. A similar plot for the emission savings is shown in Figure 8b. The chosen implementation is indicated by be the ×. This is chosen to attain both high economic and emission savings. The chosen load is 865 kW with an ammonia mass fraction 0.81. The circulation ratio is then 0.45. The exergoeconomic optimum values of pinch point temperature difference and effectiveness are: $\Delta T_{\mathrm{pp},5}$ =12.6 K, $\Delta T_{\mathrm{pp},8}$ =10.3 K, ϵ_6 =0.695 and ϵ_3 =0.860. Here the present value of the saving is 177,000 € and the yearly CO_2 emissions is reduced by a total 210 ton.

Table 6 shows the results of the exergy and exergoeconomic analysis of the chosen implementation. As seen the highest contribution to the exergy destruction in the system is caused by the compressor and the throttling valve. Both causing 22 % of the total exergy destruction. The gas cooler, absorber and desorber are the other main contributors, responsible for 17 %, 16 % and 15 % respectively. The component with the highest total cost rate is the compressor while this component has the second lowest relative cost difference. The highest relative cost difference is found in the gas cooler.

4   Discussion

The high cost rate and relative cost difference in the gas cooler is caused by the superheat of the gas exiting the compressor. This cannot be changed directly by changing the design of the gas cooler but could be reduced by the implementation of a two-stage compression. This could also reduce the exergy destruction cost of the compression. Judging from the results presented in Table 6, the HACHP could best be further improved by the implementation of a two-stage compression.

Ommen et al. [11] tested ammonia mass fractions of 0.7 and 0.9 and also found the total cost to increase with the reduction of ammonia mass fraction. The optimum pinch point temperatures found in [11] are significantly lower that those presented in the current study. This is assumed to be caused by the use of constant U-value in [11]. Hence the degradation of two-phase heat transfer due to mass

Table 6. Results of the exergy and exergoecnomic analysis of the chosen implementation

k^{th}	Component	$\dot{E}_{P,k}$ [kW]	$\dot{E}_{F,k}$ [kW]	$\dot{E}_{D,k}$ [kW]	ε_k [%]	y_k [%]	y_k^* [%]	$\dot{Z}_k$ [¢/h]	$\dot{C}_{D,k}$ [¢/h]	$f_{ex,k}$ [-]	r_k [-]
1	Compressor	187	214	27.1	87	9.2	22	415	226	0.65	0.41
2	Pump	3.12	3.79	0.670	82	0.23	0.54	8.60	5.59	0.61	0.55
3	Gas cooler	39.9	61.6	21.7	65	7.4	17	25.5	251	0.092	0.60
4	Mixer	-	-	5.30	-	1.8	4.25	21.3	-	-	-
5	Absorber	130	148.9	19.1	87	6.5	15	134	219	0.38	0.25
6	IHEX	11.5	14.8	3.26	78	1.1	2.61	32.4	37.8	0.46	0.53
7	Throttling Valve	-	-	27.5	-	9.3	22	0.00	-	-	-
8	Desorber	56.7	76.8	20.1	74	6.8	16	155	0.00	1	-

diffusion resistance is not captured. This has been shown to have an influence on both the PEC and the exergoeconomic optimum design and should be accounted for.

In the present study the 16 design conditions at which the exergoeconomic optima were determined was based only the optimization of COP. However these optimum COP points are caused by matching temperature profiles of both absorber, desorber and IHEX which consequently increases the investment in heat transfer area. As can be seen in Figure 5 the circulation ratio can deviate from the optimum value and still attain close to optimal COP values. It could therefore be of interest to evaluate the design of the heat pump with circulation ratios both above and below the optimum values. This could reduce the total cost of the HACHP further.

5 Conclusion

The implementation of HACHP in a spray drying facility has been investigated and optimized. Heat transfer and pressure drop correlations from the open literature have been gathered and implemented in the thermodynamic model of the HACHP. Cost functions based on Danish intermediate trade price have been made to assess the heat pump investment. The exergoeconomic method has been used to minimize the total cost of the HACHP. The influence of ammonia mass fraction, circulation ratio and heat pump load is also investigated. Constraints based on commercially available technologies have been imposed. The best possible implementation was found to be a 865 kW HACHP with an ammonia mass fraction of 0.81 and circulation ratio of 0.45. This resulted in an economic saving with a present value of 177.000 € and a 210 ton reduction of CO_2 emissions yearly.

Acknowledgements

Nomenclature

Abbreviations

EES engineering equation solver

HACHP hybrid absorption compression heat pump

IHEX internal heat exchanger

PEC product equipment cost

TCO total cost of operation

Symbols

$\dot{C}$	cost rate of exergy flow	€ /s
$\dot{E}$	exergy rate	kW
$\dot{m}$	mass flow rate	kg/s
$\dot{Q}$	heat Load	kW
$\dot{W}$	volume flow rate	m³/s
$\dot{W}$	work load	kW
$\dot{Z}$	levelized cost rate of capital investment and operation & maintenance	€/s
A	area	m²
b	plate corrugation depth	m
c	average cost per unit exergy	€ /kJ
e	specific exergy	kJ/kg
f	circulation ratio	-
f_{ex}	exergoeconomic factor	-
h	specific enthalpy	kJ/kg
L	length	m
N	number of -	-
p	pressure	bar
q	vapour quality	-
r	relative cost difference	-
s	specific entropy	kJ/kg-K
T	Temperature	°C (difference K)
t	plate thickness	m
U	over all heat transfer coefficient	kW/m²-K
W	Width	m
x	ammonia mass fraction	-
y	exergy destruction ratio	-
COP	coefficient of performance	-

Greek symbols

α	heat transfer coefficient	kW/m²-K
β	chevron angle	°
Δ	difference	
ϵ	effectiveness	-
η	efficiency	-
Λ	plate corrugation spacing	m
λ	conductivity	kW/m-K
ε	exergy efficiency	-

Subscripts & Superscripts

Σ	sum over all k components
D	destruction
e	electric
F	fuel
j	stream

k component

l lean

P product

r rich

v vapour

CH chemical

LMTD logarithmic mean temperature difference

PH physical

pp pinch point

vol volumetric

References

[1] Baker CGJ, McKenzie Ka. Energy Consumption of Industrial Spray Dryers. Drying Technology: An International Journal. 2005 Feb;23(1-2):365–386.

[2] Energy statistics 2012 (Original language Danish: Energistatistik 2012). Danish Energy Agency, ISBN: 978-87-93071-39-1 www.

[3] Brunin O, Fiedt M, Hivet B. Comparison of the working domains of some compression heat pumps and a compression-absorption heat pump. International Journal of Refrigeration. 1997;20(5):308–318.

[4] Jensen JK, Reinholdt L, Markussen WB, Elmegaard B. Investigation of ammonia/water hybrid absorption/compression heat pumps for heat supply temperatures above 100°C. In: International Sorption Heat Pump Conference, University of Maryland. Washington D.C; March 31 - April 2, 2014. .

[5] Osenbrück A. Refrigerating or freezing method in absorption machines (Original language German: Verfaren kalteerzeugung bei absorptions- maschinen); 1895.

[6] Altenkirch E. Vapour compression refrigeration machine with solution circuit. (Original language German: Kompressionskältemachine mit lösungskreislauf). Kältetechnik. 1950;2(10,11,12):251–259,310–315,279–284,.

[7] Lorenz H. Contributions to the assessment of cooling machines (Original language German: Beiträge zur Beurteilung von Kühlmaschinen). Z VDI. 1894;38:62–68, 98–103, 124–130.

[8] Prasertsan S, Saen-saby P. Heat Pump Dryers: Research and Development Needs and Opportunities. Drying Technology: An International Journal. 1998 Jan;16(1-2):251–270.

[9] Gungor A, Erbay Z, Hepbasli A. Exergoeconomic analyses of a gas engine driven heat pump drier and food drying process. Applied Energy. 2011;88(8):2677–2684.

[10] Chua, K J, Chou, S K, Ho, J C, Hawlader, M, N A. Heat Pump Drying : Recent Developments and Future Trends. Drying Technology: An International Journal. 2002;20(8):1579–1610.

[11] Ommen TS, Markussen CM, Reinholdt L, Elmegaard B. Thermoeconomic comparision of industrial heat pump. In: ICR 2011, August 21 - 26 - Prague, Czech Republic; 2011. .

[12] Collier JG, Thome JR. Convective Boiling and Condensation. Clarendon Press; 1994.

[13] Radermacher R, Hwang Y. Vapor Compression Heat Pumps with Refrigerant Mixtures. Mechanical Engineering. Taylor & Francis; 2005.

[14] Satapathy P. Exergy analysis of a compression–absorption system for heating and cooling applications. International Journal of Energy Research. 2008;(February):1266–1278.

[15] Hultén M, Berntsson T. The compression/absorption heat pump cycle — conceptual design improvements and comparisons with the compression cycle. International Journal of Refrigeration. 2002;25:487–497.

[16] Hultén M, Berntsson T. The compression/absorption cycle – influence of some major parameters on COP and a comparison with the compression cycle. International Journal of Refrigeration. 1999;22:91–106.

[17] Bejan A, Tsatsaronis G, Moran MJ. Thermal Design and Optimization. Wiley-Interscience publication. Wiley; 1996.

[18] Kotas TJ. The exergy method of thermal plant analysis. Butterworths; 1985.

[19] Kemp IC. Reducing Dryer Energy Use by Process Integration and Pinch Analysis. Drying Technology: An International Journal. 2005 Sep;23(9-11):2089–2104.

[20] Itard LCM, Machielsen CHM. Considerations when modelling compression/resorption heat pumps. International Journal of Refrigeration. 1994;17(7):453–460.

[21] Zheng N, Song W, Zhao L. Theoretical and experimental investigations on the changing regularity of the extreme point of the temperature difference between zeotropic mixtures and heat transfer fluid. Energy. 2013 Jun;55:541–552.

[22] Klein SA. Engineering Equation Solver Academic Professional V9.459-3D. F-Chart Software; 2013.

[23] Ibrahim OM, Klein SA. Thermodynamic Properties of Ammonia-Water Mixtures. In: ASHRAE Trans.: Symposia; 1993. p. 21, 2 1495–1502.

[24] El-Sayed YM. in Proceedings of ASME Winter Annual Meeting. vol. I-11. ASME, Chicago, 1988; 1985. p. 19–24.

[25] Thorin E. Thermophysical Properties of Ammonia Water Mixtures for Prediction of Heat Transfer Areas in Power Cycles 1. 2001;22(1).

[26] Neksa P, Rekstad H, Zakeri GR, Schiefloe PA. CO2-heat pump water heater: characteristics , system design and experimental results. International Journal of refrigeration. 1998;21(3):172–179.

[27] Qiao H, Aute V, Lee H, Saleh K, Radermacher R. A new model for plate heat exchangers with generalized flow configurations and phase change. International Journal of Refrigeration. 2013;36(2):622 – 632.

[28] Abu-Khader MM. Plate heat exchangers: Recent advances. Renewable and Sustainable Energy Reviews. 2012;16(4):1883 – 1891.

[29] Palm B, Claesson J. Plate Heat Exchangers: Calculation Methods for Single and Two-Phase Flow. Heat Transfer Engineering. 2006;27:88 – 98.

[30] Martin H. A theoretical approach to predict the performance of chevron-type plate heat exchangers. Chemical Engineering and Processing: Process Intensification. 1996;35(4):301 – 310.

[31] Táboas F, Vallès M, Bourouis M, Coronas A. Assessment of boiling heat transfer and pressure drop correlations of ammonia/water mixture in a plate heat exchanger. International Journal of Refrigeration. 2012 May;35(3):633–644.

[32] Táboas F, Vallès M, Bourouis M, Coronas A. Flow boiling heat transfer of ammonia/water mixture in a plate heat exchanger. International Journal of Refrigeration. 2010 Jun;33(4):695–705.

[33] Táboas F, Vallès M, Bourouis M, Coronas A. Pool boiling of ammonia/water and its pure components: comparison of experimental data in the literature with the predictions of standard correlations. International journal of refrigeration. 2007;30:778–788.

[34] Nordtvedt SR. Experimental and theoretical study of a compression/absorption heat pump with ammonia/water as working fluid [Ph.D. Thesis]. Norwegian University of Science and Technology; 2005.

[35] Silver L. Gas cooling with aqueous condensation: A new procedure for calculating heat transfer

coefficients. The Industial Chemist. 1947 Jun;p. 380–386.

[36] Bell KJ, Ghaly MA. An approximate generalized design method for multicomponent/partial condensers. In: 13th National Heat Transfer Conference. Denver, Colorado, USA: AIChE-ASME; 1972. .

[37] Yan Y, Lio C, Lin F. Condensation heat transfer and pressure drop of refrigerant R-134a in a plate heat exchanger. International Journal of Heat and Mass Transfer. 1999;42(6):993–1006.

[38] Bejan A. Advanced engineering thermodynamics. 3rd ed. New York: Wiley; 2006.

[39] Morosuk T, Tsatsaronis G. A new approach to the exergy analysis of absorption refrigeration machines. Energy. 2008 Jun;33(6):890–907.

[40] Tsatsaronis G, Park MH. On avoidable and unavoidable exergy destructions and investment costs in thermal systems. Energy Conversion and Management. 2002 Jun;43(9-12):1259–1270.

[41] Ahlsell Danmark ApS. Price catalog 2013. [accessed 26.09.13].

[42] H. Jessen Jörgensen A/S. Price catalog 2013. [accessed 26.09.13]..

[43] Sørensen, K. HPO R717 compressor cost. Private communication 2013..

[44] Zamjlrescu C. Modeling and optimization of an ammonia-water compression-resorption heat pumps with wet compression. Trans Can Soc Mech Eng. 2009;33(1):75–88.